文章编号:1006-9941(2020)04-0336-08

Combustion Performance of Fe_2O_3-containing Nanothermites Prepared by Ball Milling Method

JIANG Ai-feng, XIA De-bin, LI Meng-ru, LIN Kai-feng, QIANG Liang-sheng, LI Jia-he, FAN Rui-qing, YANG Yu-lin

(*MIIT Key Laboratory of Critical Materials Technology for New Energy Conversion and Storage, School of Chemistry and Chemical Engineering, Harbin Institute of Technology, Harbin* 150001, *China*)

Abstract: Various preparation methods have been widely explored to improve the combustion performance of nanothermites in recent years. In this work, two kinds of Fe_2O_3-containing nanothermites were successfully prepared by *in-situ* ball milling method and conventional ultrasonic blending method respectively. The morphologies and performance of as-prepared products have been fully characterized by thermogravimetric analysis (TGA), X-ray diffraction (XRD), contact angle tests, scanning electron microscopy (SEM), high-speed imaging experiments and infrared temperature measurement. The results show that the Fe_2O_3-doped nanothermites via *in-situ* ball milling method exhibit better performance than that made by ultrasonic blending method. The optimal nanothermites with 17% Fe_2O_3 doped amount possess the maximum mass gain percentage of 13.1% per 100 ℃. Compared with the products made by ultrasonic blending method, the heating voltage and initial combustion temperature of *in-situ* ball milled nanothermites decrease to 12 V and 600 ℃, respectively. In addition, the combustion flame of *in-situ* ball milled nanothermites is more stable and homogeneous than the corresponding one.

Key words: nanothermites; *in-situ* ball milling; ultrasonic blending; contact angle; combustion flame

CLC number: TJ55; O69 **Document code:** A **DOI:** 10.11943/CJEM2019071

1 Introduction

Thermites, commonly composed of metal and metal oxide[1-8], is one major kind of energetic materials (EMs) and extremely attracts researcher's growing attentions due to their high energy densities, rapid reaction rate, ready availability and wide range of tunability[9-13]. Especially, nanothermites assembled with nano-scale particles remarkably reduces the mass diffusion distance and promotes the intimate mixing[14-17] of the fuels and oxidizers, and yields an enhanced performance. For example, Aumann et al.[18] presented that Al/MoO_3 nanocomposites possess improved energy release rate, which was attributed to the nano-scaled particle sizes. Beside the particle size controlling, the well mixture of fuels and oxidizers should be another key point to the high performance of thermites. Therefore, various methods have been employed to prepare the nanothermites, such as ultrasonic blending method[19-21], physical vapor deposition method (PVD)[22-24] and sol-gel method[25-26]. However, these methods are still suffered from the low-yield, high-cost and complicated process disadvantages.

Ball milling technique[27-29] is an another typical

Received Date: 2019-03-13; **Revised Date:** 2019-04-21

Published Online: 2019-11-20

Project Supported: SFAC (6141B0626020201, 6141B0626020101), National Natural Science Foundation of China (21571042, 51603055, 21873025), the Natural Science Foundation of Heilongjiang Province (QC2017055), the China Postdoctoral Science Foundation (2016M601424, 2017T100236), the Postdoctoral Foundation of Heilongjiang Province (LBH-Z16059).

Biography: JIANG Ai-feng (1992-), male, doctoral candidate, majoring in the study of energetic materials. e-mail: jiangaifenghit@163.com

Corresponding author: YANG Yu-lin (1969-), male, professor, majoring in the study of energetic materials. e-mail: ylyang@hit.edu.cn; FAN Rui-qing (1970-), female, professor, majoring in the study of supramolecular coordination polymer materials.
e-mail: fanruiqing@hit.edu.cn

引用本文:姜艾锋,夏德斌,李梦茹,等.球磨法制备Fe_2O_3掺杂纳米铝热剂及其燃烧性能[J].含能材料,2020,28(4):336-343.
JIANG Ai-feng, XIA De-bin, LI Meng-ru, et al. Combustion Performance of Fe_2O_3-containing Nanothermites Prepared by Ball Milling Method[J]. *Chinese Journal of Energetic Materials (Hanneng Cailiao)*, 2020, 28(4):336-343.

method for preparing the composite samples, in which particles can be refined *via* mechanical forces. The products can achieve the overall-increased surface area and controllable structural defects by ball milling method, which enhance the chemical activity. Therefore, the well-mixed thermites with high density could be obtained cost-effectively and massive productively through ball milling method. However, the particle size controlling together with relatively small output is still a big problem for this method. Very recently, aluminum particles with uniform nano-sized by modified ball milling method were successfully prepared[30].

Based on this experience, a series of Fe_2O_3-containing nanothermites with different oxide content were successfully prepared by *in-situ* ball milling method on a large scale. At the same time, the common ultrasonic blending method has also been utilized to prepare the nanothermites with the same doped amounts for comparison. The mixing uniformity, thermal behavior and hydrophobicity of as-prepared products were investigated by a series of measurements and calculations. Additionally, the combustion performances between the composites prepared *via* two methods were also deeply discussed.

2 Experiments

2.1 Reagents and Instruments

The 4A molecular sieve was purchased from Sinopharm Chemical Reagent Co., Ltd. and treated by calcinating at 400 ℃ for 2 h in a muffle furnace. Dimethyl Sulfoxide (DMSO) was obtained from Aladdin and pre-purified *via* decompressing distillation technique by refluxing with calcium hydride (CaH_2) under a dry nitrogen (N_2) atmosphere for 24 h to keep anhydrous and oxygen free. Afterwards, the distilled DMSO solvent mixed with activated 4A molecular sieve under magnetic stirring for 8 h for deeply purified. Micron aluminum powders were received from Anshan Industry Fine Aluminum Powders Company Limited. Ferric oxide (Fe_2O_3) was purchased from Innochem. CaH_2 and trimethoxy(vinyl) silane (A171) were obtained from Alfa Aesar. Cyclohexane and ammonium chloride (NH_4Cl) were obtained from Aladdin.

2.2 Methods

2.2.1 Sample preparation

The loading, sampling and covering processes were all operated in a glovebox under high purity N_2. The ball milling method was carried out by QM-3SP4 planetary ball-mill in the steel vials and the milling mediums were steel balls with a diameter of 5 mm. The mixture of micron aluminum powders, Fe_2O_3, and NH_4Cl, and steel balls with 1∶50 mass ratio, were all added into the steel vials and sealed tightly, then ball milling for 14 h. In addition, the added mass loading of Fe_2O_3 is 1%, 5%, 9%, 13%, 17% and 21% of micron aluminum powders, respectively. After ball milling process, all products were washed by purified DMSO for 3 times to remove NH_4Cl.

Then, the mixture of 0.5 mL A171 and 100 mL cyclohexane were added into a two-neck flask as primed solution. Afterwards, 10 g ball-milled products were added into well-mixed primed solution and stirring for one hour at 80 ℃. The separation of solids and liquids were executed by vacuum filtration and washed 3 times by using cyclohexane. Finally, the products were dried in the vacuum drying oven for an hour at room temperature. The ultrasonic blending method was also performed as follows: the mixture of 10 g ball-milled aluminum nanoparticles and 100 mL purified cyclohexane were added to a two-neck flask. Then, various Fe_2O_3 (1%~21%) powders and 0.5 mL A171were added in afterwards. Subsequently, the suspension was continued ultrasonic dispersed for 1 h and the solution was removed via vacuum filtration by cyclohexane washing for 3 times. Finally, the samples were dried with the same conditions.

2.2.2 Experimental Measurements

The crystalline of as-prepared composites were performed by X-ray powder diffraction (XRD) analysis (Cu Kα) using a PANalytical Empyrean instru-

ment with a range of 10° to 90°. Thermogravimetric analysis (TGA) was detected by SDT Q600 from room temperature to 850 ℃ at the heating rate of 10 ℃·min^{-1} under air flow. High speed imaging images were measured by Germany Dantec Dynamics high speed camera at a frame rate of 1500 fps and 640×480 resolution. The combustion flames temperature was simultaneously measured by Germany DIAS Infrared Systems under air atmosphere. Samples were treated by ultrasonicating in cyclohexane for 30 min and adhered on a ~10 mm long Ni-Cr wire (220 μm). The metal wire was heated by energization and controlled by changing the voltage. Contact angles was conducted via JC2000C from Shanghai Zhongchen. Scanning electron microscope (SEM) were employed by Hitachi SU 8000HSD.

3 Results and discussion

3.1 Particles structure

In order to verify the structures of as-prepared nanothermites by ball milling method, the XRD was conducted and the results shown in Fig.1a. The XRD patterns of samples doped with 1% and 5% Fe_2O_3 mainly shows the aluminum peaks (2θ =38.47°, 44.74°, 65.13°, 78.23° and 82.44°). In addition, the weak diffraction peaks at 2θ=33.12° and 35.61° are presented, which could be attributed to the presence of Fe_2O_3. When the doped amounts are gradually increased up to 21%, the XRD patterns obviously identified the existence of aluminum and Fe_2O_3, and the intensity of the Fe_2O_3 diffraction peaks increased by doped amounts. The similar results were also observed in the patterns of nanothermites prepared by ultrasonic blending method (Fig. 1b). These results exhibit that Fe_2O_3 are successfully doped in aluminum nanoparticles prepared by the two methods.

3.2 Thermal stability

In order to compare the oxidation effect of Fe_2O_3 on aluminum nanoparticles prepared by *in-situ* ball milling method and ultrasonic blending method, the TGA measurements are conducted (Fig. 2).

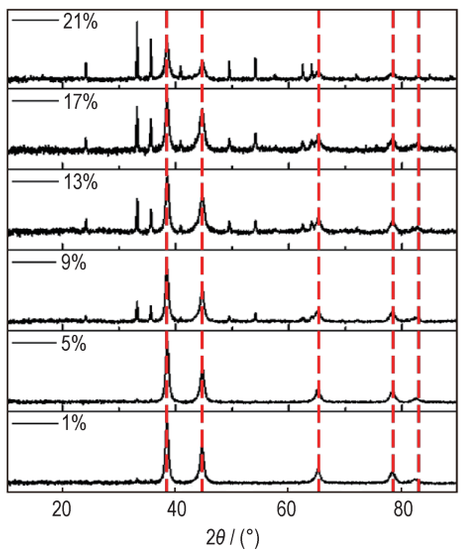

a. *in-situ* ball milling method

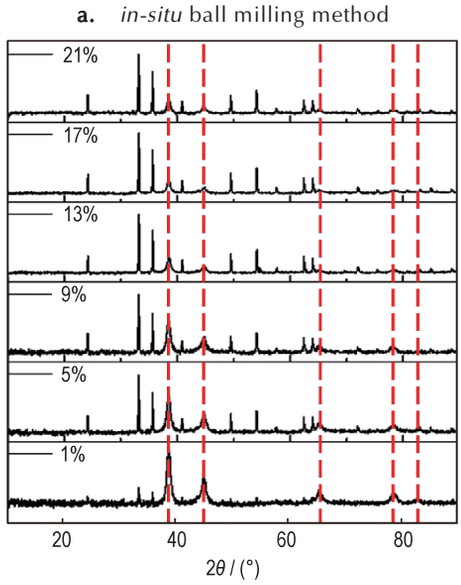

b. ultrasonic blending method

Fig. 1 X-ray diffraction (XRD) patterns of nanothermites doped with different amounts of Fe_2O_3 *via* different methods (Note: the peaks marked by red dotted lines represent Al peaks and the unmarked peaks are all Fe_2O_3 peaks)

With regard to the nanothermites prepared by *in-situ* ball milling method, the initial oxidation temperature of all compisites gradually decreases as the Fe_2O_3 doped amounts increase from 1% to 17%, indicating the addition of Fe_2O_3 is indeed able to accelerate the oxidation rate of aluminum nanoparticles. However, when the doped amount increased to 21%, the initial oxidation temperature is no obvious change and the mass gain slightly decreased. Therefore, the addition of Fe_2O_3 may bring about two ef-

fects, decreasing in aluminum content and accelerating the oxidation rate of aluminum nanoparticles. As a consequence, the optimal Fe_2O_3 doped amount of nanothermites prepared by *in-situ* ball milling method for accelerating the oxidation rate is 17%. As for the nanothermites prepared by ultrasonic blending method, the optimal product for promoting oxidation of aluminum nanoparticles is the nanothermites doped with 5% Fe_2O_3 (Fig. 2b) and the oxidation rate gradually decreases as the doped amounts increase when the Fe_2O_3 doped amounts exceed 9%, indicating that the mixing degree of the nanothermites prepared by the ultrasonic blending method is not so similar as that of *in-situ* ball milling method.

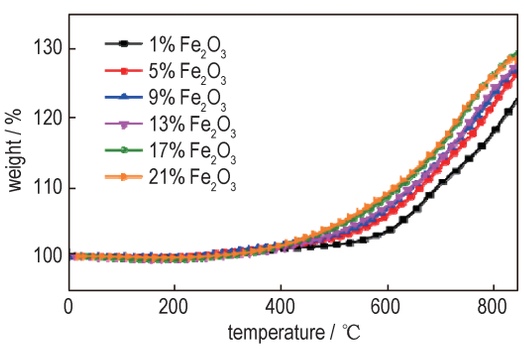

a. *in-situ* ball milling method

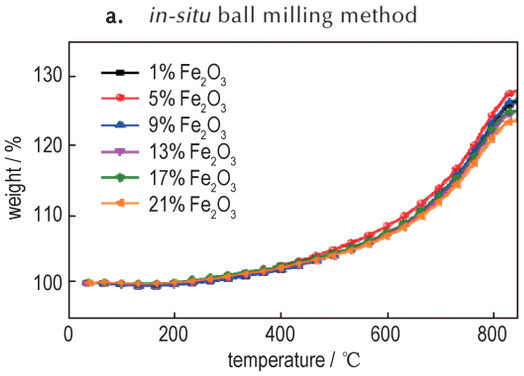

b. ultrasonic blending method

Fig. 2 TGA curves of nanothermites doped with different amounts of Fe_2O_3 *via* two methods

To compare and theoretically analyze the rising rate of the TGA curves of nanothermites obtained from two methods, fitting functions were employed by Origin software[31] and the results are shown in Fig.3, Fig.4 and Table 1. The fitting functions of *in-situ* ball-milled nanothermites and ultrasonic-blended nanothermites were set to $f(Bx)$ and $f(Sx)$, respectively, and the fitting curves derivatives were set to $\dot{f}(Bx)$, and $\dot{f}(Sx)$, respectively. Given that the curves fitting and calculation processes of different doped amounts of Fe_2O_3 are similar, so the TGA curves of doped 17% Fe_2O_3 ball-milled composite and doped 5% Fe_2O_3 ultrasonic-blended composite were selected and investigated. The functions of the fitting curves are presented as follows:

$$f(Bx) = 7.510 \times 10^{-8}x^3 - 1.798 \times 10^{-5}x^2 - 0.00143x + 100.038$$

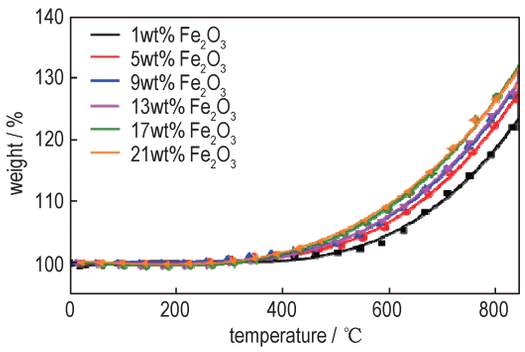

Fig. 3 TGA fitting curves of nanothermites doped with different amounts of Fe_2O_3 prepared by *in-situ* ball milling method.

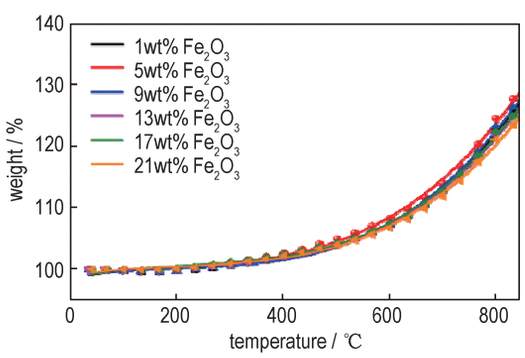

Fig. 4 TGA fitting curves of nanothermites doped with different amounts of Fe_2O_3 prepared by ultrasonic blending method.

Table 1 Maximum rising rate (850 ℃) of TGA fitting curves derivatives of nanothermites prepared by *in-situ* ball milling method and ultrasonic blending method %

Fe_2O_3 mass fraction / %	maximum mass gain percentage per 100 ℃	
	ball milling method	ultrasonic blending method
1	11.8	12.0
5	12.9	12.2
9	13.0	12.2
13	12.9	11.4
17	13.1	11.4
21	12.4	10.8

$$f(Sx) = 9.313 \times 10^{-8}x^3 - 5.652 \times 10^{-5}x^2 + 0.0165x + 98.603$$

For the purpose of obtaining the rising rates of the fitting curves, the derivative functions of above-mentioned functions are calculated as follows:

$$\dot{f}(Bx) = 2.253 \times 10^{-7}x^2 - 3.596 \times 10^{-5}x - 0.00143$$

$$\dot{f}(Sx) = 2.794 \times 10^{-7}x^2 - 1.130 \times 10^{-4}x - 0.0165$$

Therefore, the maximum rising rate of TGA fitting curves were calculated at 850 ℃ and the oxidation rates of all samples were reflected by mass gain percentage per 100 ℃. Obviously, the maximum mass gain percentage per 100 ℃ of optimal *in-situ* ball-milled nanothermites was 13.1%. The maximum mass gain percentage per 100 ℃ of ultrasonic-blended nanothermites was only 12.2%, indicating the two fitting curves with 5% and 9% doped composites shown similar oxidation rates. However, the mass gain of the 5% doped composite is higher than that of 9%, illustrating the oxidation degree of nanothermites doped with 5% Fe_2O_3 is more complete than that of nanothermites doped with 9% Fe_2O_3.

As a consequence, the optimal doped amounts of nanothermites prepared by the two methods were 17% and 5% for ball-milled and ultrasonic-blended composites, respectively, and the *in-situ* ball-milled nanothermites possess higher oxidation rate in comparison with the ultrasonic-blended nanothermites, which is consistent with the results presented by TGA curves.

3.3 Microscopic morphology

To exhibit the particles size, element distribution and microscopic morphology of nanothermites prepared by the two methods, scanning electron microscope (SEM) and mapping scanning of energy dispersive spectrometer (EDS) analysis were conducted and the results are presented in Fig.5.

Obviously, aluminum and iron elements in the prepared nanothermites are both displayed clearly, (Fig.5a and Fig.5b), which is in agreement with the XRD results. The enlarged SEM image and schematic diagram of *in-situ* ball-milled nanothermites doped with 17% Fe_2O_3 are shown in Fig.5c and Fig.5e, illustrating the ball-milled particles are indeed nano-sized particles and spherical. However, the self-agglomeration phenomenon can be observed in the enlarged SEM image and schematic diagram of ultrasonic-blended nanothermites, indicating uneven mixing of Al and Fe_2O_3 particles (Fig.5d and Fig.5f) and greatly reduced mixing intimacy. As a consequence, Al and Fe_2O_3 particles of ball-milled nanothermites dispersed more uniformly than that of ultrasonic-blended nanothermites.

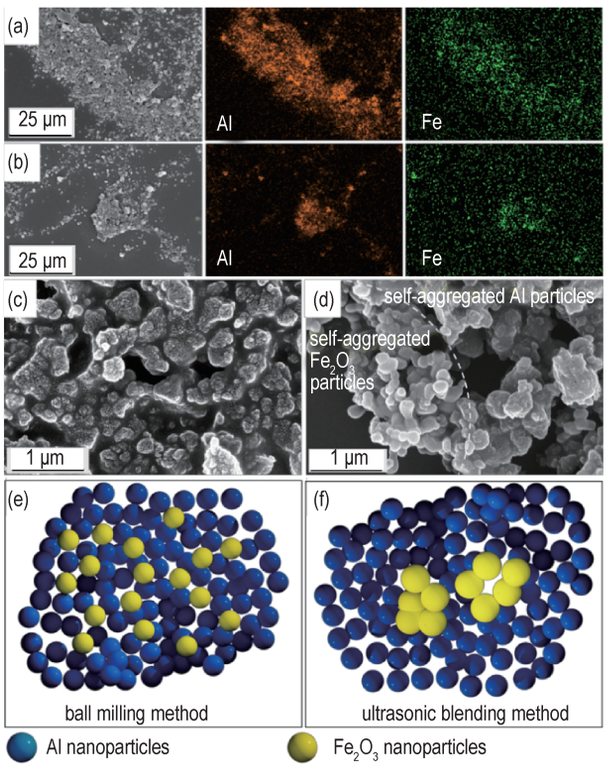

Fig. 5 Microscopic morphology and element distribution of *in-situ* ball-milled and ultrasonic-blended nanothermites: (a) Element distribution of *in-situ* ball-milled nanothermites doped with 17 % Fe_2O_3 from EDS mapping; (b) Element distribution of ultrasonic-blended nanothermites doped with 17 % Fe_2O_3 from EDS mapping; (c) corresponding SEM images of *in-situ* ball-milled nanothermites doped with 17 % Fe_2O_3; (d) corresponding SEM images of ultrasonic-blended nanothermites doped with 5 Fe_2O_3; (e) Schematic diagram of *in-situ* ball-milled nanothermites doped with 17 % Fe_2O_3 and (f) Schematic diagram of ultrasonic-blended nanothermites doped with 5 % Fe_2O_3.

3.4 Hydrophobicity

The hydrophobicity of nanothermites prepared by two methods were investigated and the contact angles were detected and the results presented in Fig.6.

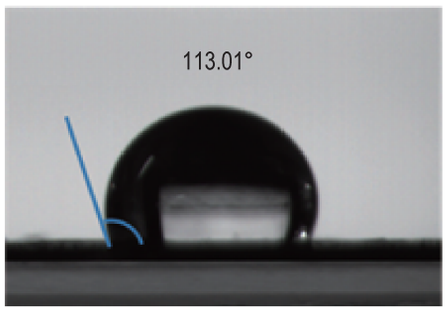

a. *in-situ* ball milling method (17% Fe_2O_3)

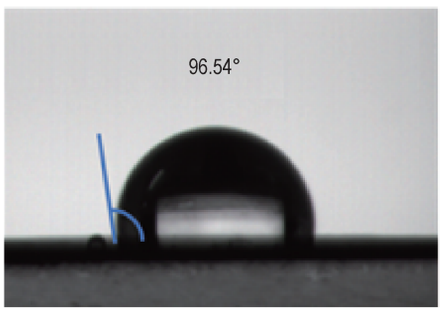

b. ultrasonic blending method (5% Fe_2O_3)

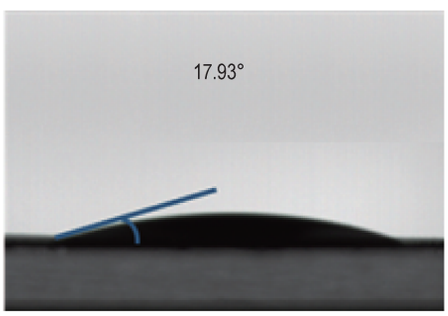

c. Fe_2O_3 particles

Fig. 6 Contact angles of nanothermites doped different amounts of Fe_2O_3 *via* different methods.

Clearly, the contact angles of nanothermites obtained from ball milling method, ultrasonic blending method and pristine Fe_2O_3 are 113.01°, 96.54° and 17.93°, respectively. The result could be ascribed to the exposure of Fe_2O_3 nanoparticles to the surrounding atmosphere and water, stemming from the uneven mixing of Al and Fe_2O_3 particles. In contrast, the contact angle of *in-situ* ball-milled nanothermites doped with 17% Fe_2O_3 (113.01°) is much larger than that of the ultrasonic-blended composite, indicating that *in-situ* ball-milled composites possess better hydrophobicity than that os ultrasonic-blended composites. Therefore, *in-situ* ball-milled nanothermites are more conducive to preservation in comparison to ultrasonic blended nanothermites.[32]

3.5 Combustion performance

To obtain the real-time flame temperature and combustion phenomena of nanothermites prepared by the two methods, infrared temperature measurement and high-speed imaging experiments were conducted on two compisites.

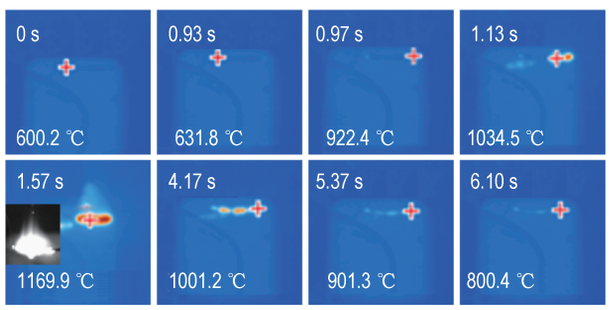

a. *in-situ* ball milling method (17% Fe_2O_3, 12 V)

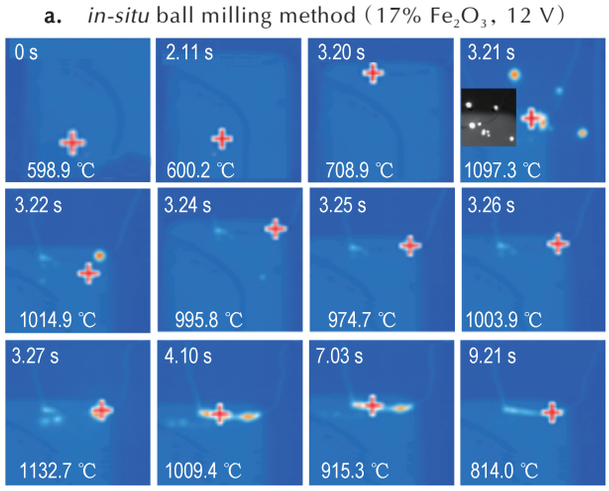

b. ultrasonic blending method (5% Fe_2O_3, 12V and 15 V)

Fig. 7 Images of real-time infrared temperature measurement of nanothermites prepared *via* different methods. (Note: The cross symbols (+) represent the tracked automatically highest temperature points.)

As shown in Fig.7, the initial heating voltage is 12 V and the initial heating temperature is around 600 ℃. For the *in-situ* ball-milled composite, the temperature slowly increases to approximately 630 ℃, indicating the passivation agent starts to rupture and partial aluminum nanoparticles of nanothermites begin to be oxidized. Then the temperature rapidly increases over 900 ℃ within 0.4 s, pointing to the oxidation of massive aluminum nanoparticles of nanothermites and heat release. Hereafter, the temperature continued to increase up to about 1170 ℃ and the combustion flame is stable. In con-

trast, as for the ultrasonic-blended compoiste, it is difficult to be ignited at 12 V voltage, so higher voltage (15 V) was applied for the ignition. At this time, the composite rapidly reacts and the temperature rises up to nearly 1100 ℃. With the rapid increase of temperature, the nanothermites prepared by ultrasonic blending method exist the phenomenon of particle sputtering and the temperature dropped rapidly or even fell below 1000 ℃. This is because the aluminum nanoparticles and the Fe_2O_3 contained in nanothermites prepared by ultrasonic blending method are seriously self-aggregated, resulting in inhomogeneous mixing and unstable combustion. Consequently, the initial combustion temperature of the nanothermites prepared by *in-situ* ball milling method is lower than that of the nanothermites prepared *via* ultrasonic blending method, and the combustion flame is more homogeneous and stable.

4 Conclusions

(1) The Fe_2O_3 powders and aluminum particles of nanothermites prepared *via* ball milling method are mixed more evenly, nevertheless, the nanothermites prepared by ultrasonic blending method exist clearly distinguished respective agglomerated aluminum particles and Fe_2O_3 particles.

(2) The contact angle of the nanothermites prepared by *in-situ* ball milling method is 113.01°, which is significantly larger than that of corresponding ultrasonic blending method (96.54°). With the optimal doped Fe_2O_3 amount (17%) by *in-situ* ball milling, the maximum mass gain percentage per 100 ℃ is 13.1%, which is larger than that for ultrasonic-blended doped 5% Fe_2O_3 product (12.2%).

(3) The *in-situ* ball milled nanothermites could be ignited at lower heating voltage (12 V) and lower initial combustion temperature (~ 600 ℃) than those of ultrasonic-blended nanothermites (15 V and ~ 700 ℃), and the combustion flame is more stable and homogeneous. This investigation is expected to promote the development of nanothermites.

References:

[1] Luo Q, Long X, Nie F, et al. The safety properties of a potential kind of novel green primary explosive: Al/Fe_2O_3/RDX nanocomposite [J]. *Materials*, 2018, 11(10): 1-10.

[2] Nguyen Q, Huang C, Schoenitz M, et al. Nanocomposite thermite powders with improved flowability prepared by mechanical milling [J]. *Powder Technology*, 2018, 327: 368-380.

[3] Sahoo S K, Danali S M, Arya P R. Ignition behavior of Al/Fe2O3 metastable intermolecular composites [J]. *International Journal of Engineering Science*, 2017, 3(11): 61-71.

[4] Wu J, Xue S, Bridges D, et al. Electrophoretic deposition and thermo-chemical properties of Al/Fe2O3 nanothermite thick films [J]. *Engineered Science*, 2018, 4: 52-64.

[5] Deng S, Jiang Y, Huang S, et al. Tuning the morphological, ignition and combustion properties of micron-Al/CuO thermites through different synthesis approaches [J]. *Combustion and Flame*, 2018, 195: 303-310.

[6] Rossi C. Engineering of Al/CuO reactive multilayer thin films for tunable initiation and actuation [J]. *Propellants, Explosives, Pyrotechnics*, 2018, 44(1): 94-108.

[7] Sui H, LeSergent L, Wen J Z. Diversity in addressing reaction mechanisms of nano-thermite composites with a layer by layer structure [J]. *Advanced Engineering Materials*, 2018, 20(3): 1700822.

[8] Zakiyyan N, Wang A, Thiruvengadathan R, et al. Combustion of aluminum nanoparticles and exfoliated 2D molybdenum trioxide composites [J]. *Combustion and Flame*, 2018, 187: 1-10.

[9] Chen Y, Zhang W, Yu C, et al. Controllable synthesis of NiCo2O4/Al core-shell nanowires thermite film with excellent heat release and short ignition time [J]. *Materials Design*, 2018, 155(5): 396-403.

[10] Jian G, Piekiel N W, Zachariah M R. Time-resolved mass spectrometry of nano-Al and nano-Al/CuO thermite under rapid heating: a mechanistic study [J]. *Journal of Physical Chemistry C*, 2012, 116(51): 26881-26887.

[11] Sullivan K, Young G, Zachariah M R. Enhanced reactivity of nano-B/Al/CuO MIC's [J]. *Combustion and Flame*, 2009, 156(2): 302-309.

[12] Sullivan K, Zachariah M R. Simultaneous pressure and optical measurements of nanoaluminum thermites: investigating the reaction mechanism [J]. *Journal of Propulsion and Power*, 2010, 26(3): 467-472.

[13] Wang H, Jian G, Egan G C, et al. Assembly and reactive properties of Al/CuO based nanothermite microparticles [J]. *Combustion and Flame*, 2014, 161(8): 2203-2208.

[14] Prakash A, McCormick A V, Zachariah M R. Tuning the reactivity of energetic nanoparticles by creation of a core-shell nanostructure [J]. *Nano Letters*, 2005, 5(7): 1357-1360.

[15] Zhou L, Piekiel N, Chowdhury S, et al. Time-resolved mass spectrometry of the exothermic reaction between nanoaluminum and metal oxides: the role of oxygen release [J]. *Journal of Physical Chemistry C*, 2010, 114: 14269-14275.

[16] Chowdhury S, Sullivan K, Piekiel N, et al. Diffusive vs explosive reaction at the nanoscale [J]. *Journal of Physical Chemistry C*, 2010, 114(20): 9191-9195.

[17] Sullivan K T, Piekiel N W, Wu C, et al. Reactive sintering:

An important component in the combustion of nanocomposite thermites [J]. *Combustion and Flame*, 2012, 159(1): 2-15.
[18] Aumann C E. Oxidation behavior of aluminum nanopowders [J]. *Journal of Vacuum Science & Technology B*, 1995, 13(3): 1178-1183.
[19] Saceleanu F, Idir M, Chaumeix N, et al. Combustion characteristics of physically mixed 40 nm aluminum/copper oxide nanothermites using laser ignition [J]. *Frontiers in Chemistry*, 2018, 6: 1-10.
[20] Su H, Zhang J, Du Y, et al. New roles of metal - organic frameworks: Fuels for aluminum-free energetic thermites with low ignition temperatures, high peak pressures and high activity [J]. *Combustion and Flame*, 2018, 191: 32-38.
[21] Wu T, Wang X, DeLisio J B, et al. Carbon addition lowers initiation and iodine release temperatures from iodine oxide-based biocidal energetic materials [J]. *Carbon*, 2018, 130: 410-415.
[22] Yu C, Zhang W, Gao Y, et al. The super-hydrophobic thermite film of the Co3O4/Al core/shell nanowires for an underwater ignition with a favorable aging-resistance [J]. *Chemical Engineering Journal*, 2018, 338(15): 99-106.
[23] Zheng Z, Zhang W, Yu C, et al. Integration of the 3DOM Al/Co3O4 nanothermite film with a semiconductor bridge to realize a high-output micro-energetic igniter [J]. *RSC Advances*, 2018, 8(5): 2552-2560.
[24] Abdallah I, Zapata J, Lahiner G, et al. Structure and chemical characterization at the atomic level of reactions in Al/CuO multilayers [J]. *ACS Applied Energy Materials*, 2018, 1(4): 1762-1770.
[25] Hübner J, Klaumünzer M, Comet M, et al. Insights into combustion mechanisms of variable aluminum-based iron oxide/-hydroxide nanothermite [J]. *Combustion and Flame*, 2018, 184: 186-194.
[26] Gao K, Wang L, Li G, et al. Preparation and characterization of the AP/Al/Fe_2O_3 ternary nano-thermites [J]. *Journal of Thermal Ananlysis and Calorimetry*, 2014, 118: 43-49.
[27] Liu X, Schoenitz M, Dreizin E L. Preparation, ignition, and combustion of magnesium-calcium iodate reactive nano-composite powders [J]. *Chemical Engineering Journal*, 2019, 359: 955-962.
[28] Monk I, Schoenitz M, Dreizin E L. The effect of heating rate on combustion of fully dense nanocomposite thermite particles [J]. *Combustion Science and Technology*, 2018, 190(2): 203-221.
[29] Hobosyan M, Martirosyan K S, Lyshevski S E. Design and evaluations of 3D-printed microthrusters with nanothermite propellants [J]. *2018 IEEE 38th International Conference on Electronics and Nanotechnology*, 2018, 478-482.
[30] Jiang A F, Wang F, Xia D B, et al. Aluminum nanoparticles manufactured using a ball-milling method with ammonium chloride as a grinding aid: achieving energy release at low temperature [J]. *New Journal of Chemistry*, 2019, 43: 1851-1856.
[31] Moghadam R Z, Ehsani M H, Dizaji H R, et al. Modification of hydrophobicity properties of diamond like carbon films using glancing angle deposition method [J]. *Materials Letters*, 2018, 220: 301-304.
[32] Wang Y, Hu Y, Cao Z Y, et al. Application of Origin software to experimental data fitting in chemical engineering principle [J]. *Experimental Technology and Management*, 2010, 27(1): 86-88.

球磨法制备 Fe_2O_3 掺杂纳米铝热剂及其燃烧性能

姜艾锋,夏德斌,李梦茹,林凯峰,强亮生,李佳贺,范瑞清,杨玉林
(哈尔滨工业大学化学化工学院 新能源转换与储存关键材料技术重点实验室, 黑龙江 哈尔滨 150001)

摘　要: 近年来,广大学者已经研究了多种方法来制备纳米铝热剂和改善其燃烧性能。本研究分别采用原位球磨法和超声共混法成功制备了两种含 Fe_2O_3 纳米铝热剂。通过热重分析(TGA)、函数拟合、X射线衍射(XRD)、接触角测试、扫描电子显微镜测试(SEM)、高速摄像实验和红外温度测量充分表征了所制备产品的形貌和性能。结果表明,通过原位球磨法制备的 Fe_2O_3 掺杂的纳米铝热剂的性能要优于超声共混法制备的铝热剂。通过对 Fe_2O_3 掺杂量的筛选发现,原位球磨法制备的纳米铝热剂的 Fe_2O_3 最优掺杂量为17%,该产物每100 ℃最大增重百分比为13.1%。与超声共混法制备的纳米铝热剂相比,原位球磨法制备的纳米铝热剂的加热电压和初始燃烧温度分别降至12 V和600 ℃。此外,原位球磨法制备的纳米铝热剂的燃烧火焰更稳定和均匀。

关键词: 纳米铝热剂;原位球磨;超声共混;接触角;燃烧火焰
中图分类号: TJ55;O69　　**文献标志码:** A　　**DOI:**10.11943/CJEM2019071
(责编:姜　梅)